Nucl Eng Technol 47 (2015) 461–471

Available online at www.sciencedirect.com

ScienceDirect

journal homepage: http://www.journals.elsevier.com/nuclear-engineering-and-technology/

Original Article

INTEGRATED SOCIETAL RISK ASSESSMENT FRAMEWORK FOR NUCLEAR POWER AND RENEWABLE ENERGY SOURCES

*SANG HUN LEE and HYUN GOOK KANG**

Department of Nuclear and Quantum Engineering, KAIST 291 Daehak-ro, 373-1 Guseong-dong, Yuseong-gu, Daejeon 305-701, Republic of Korea

ARTICLE INFO

Article history:
Received 13 October 2014
Received in revised form
13 January 2015
Accepted 14 January 2015
Available online 27 March 2015

Keywords:
Nuclear power
Probabilistic risk assessment
Renewable energy sources
Societal risk

ABSTRACT

Recently, the estimation of the social cost of energy sources has been emphasized as various novel energy options become feasible in addition to conventional ones. In particular, the social cost of introducing measures to protect power-distribution systems from power-source instability and the cost of accident-risk response for various power sources must be investigated. To account for these risk factors, an integrated societal risk assessment framework, based on power-uncertainty analysis and accident-consequence analysis, is proposed. In this study, we applied the proposed framework to nuclear power plants, solar photovoltaic systems, and wind-turbine generators. The required capacity of gas-turbine power plants to be used as backup power facilities to compensate for fluctuations in the power output from the main power source was estimated based on the performance indicators of each power source. The average individual health risk per terawatt-hours (TWh) of electricity produced by each power source was quantitatively estimated by assessing accident frequency and the consequences of specific accident scenarios based on the probabilistic risk assessment methodology. This study is expected to provide insight into integrated societal risk analysis, and can be used to estimate the social cost of various power sources.

1. Introduction

After the Fukushima Daiichi nuclear power plant (NPP) accident, the Japanese government published a report in which the unit electricity generation costs of various power sources are estimated [1]. This report suggests that the unit value of nuclear power generation will be 8.9 yen/kWh (11.4 U.S. cents/kWh), including the social cost of 1.6 yen/kWh (2.0 U.S. cents/kWh), by the year 2020. Regarding renewable energy, by the year 2020, the unit value of onshore wind power is estimated to reach 9.3–17.3 yen/kWh (11.9–22.2 U.S. cents/kWh) and that of residential solar power generation is estimated to reach 12.0–13.9 yen/kWh (15.4–17.8 U.S. cents/kWh); whereas the social cost of wind-turbine generators (WTGs) and solar

* *Corresponding author.*
E-mail address: hyungook@kaist.ac.kr (H.G. Kang).

http://dx.doi.org/10.1016/j.net.2015.01.009
1738-5733/Copyright © 2015, Published by Elsevier Korea LLC on behalf of Korean Nuclear Society.

photovoltaic (PV) systems is estimated to be 0 yen/kWh. The additional expenditure of providing measures to protect the power-distribution network from power-source instability and that of accident-risk response for renewable energy sources were not considered; however, these social costs must be considered for proper electricity generation cost estimation.

In general, solar PV systems and WTGs are considered to be intermittent energy sources, whose power output is not continuously available because of certain external factors that are outside direct control. The effective use of such intermittent energy sources in an electric power grid for utility purposes usually relies on the use of backup power to compensate for the irregular fluctuations in output from the intermittent sources. When one considers the external cost of additional backup power installations to compensate for the deficiencies in the energy supplied by various sources, the electricity generation cost can increase, depending on the performance or reliability of each source.

In terms of the cost of accident-risk response, concerns have been raised regarding the potential public risks of not only NPPs but also WTGs and solar PV systems. The primary concern regarding NPPs is that radioactive fission products may be released into the environment and may pose a radiation hazard to the adjacent public in the case of a severe accident scenario [2]. Although renewable energy sources generally appear to generate no potential hazards, several studies have highlighted the potential risk of an accidental fire in a PV array theoretically releasing toxic substances into the environment, and turbine blades can be thrown to nearby sites in the case of blade-failure accidents in WTGs, endangering anyone living near the wind farms [3,4].

To account for these risks in the estimation of the social cost of various power sources, an integrated societal risk assessment framework for NPPs, WTGs, and solar PV systems, based on power-uncertainty analysis and accident-consequence analysis, is proposed in this paper. For the power-uncertainty analysis, the deficiencies in power output caused by the inadequate performance of a given power source are assumed to be compensated for through the immediate use of gas-turbine power plants. For the accident-consequence analysis, various possible accident scenarios were considered, including a hypothetical NPP accident, a fire-related incident within a solar PV system, and the whole-blade failure of a utility-scale wind turbine. This study is expected to provide insights into integrated societal risk analysis and will be used as the basis for estimating the social costs of various energy sources.

2. Proposed framework

2.1. Power-uncertainty analysis

This study looks at a hybrid energy system consisting of a main power source, in combination with auxiliary gas-turbine power plants as the backup power source, to supply electricity when the main power source does not generate sufficient energy to satisfy the load demand, or is not available during outage periods. The required annual production of the hybrid energy system can be calculated as the sum of the actual annual power output of each power source and the required annual power output from the gas:

$$W_r = \mu_i C_{p,i} W_i + W_g \tag{1}$$

where W_r is the required annual energy production of the hybrid energy system, W_g is the required annual power output from the gas turbines, and μ_i, $C_{p,i,}$ and W_i represent the availability factor (AF), capacity factor (CF), and rated annual energy output of the main power source, respectively. To ensure a reliable supply from this system, the annual production of the hybrid energy system must be equal to the rated annual power output of the main power source, and thus the annual power production required of the gas turbines that must be installed can be derived as follows:

$$W_r = W_i \tag{2}$$

$$W_g = (1 - \mu_i C_{p,i}) W_i \tag{3}$$

Using Eq. (3), the electricity generation cost can then be derived as the sum of the yearly electricity generation cost of the main power source and the yearly electricity generation cost of the required gas turbines, divided by the annual rated power production of the energy source

$$c_i = \frac{c_{e,i} W_i + c_g W_g}{W_i} = c_{e,i} + c_g \frac{W_g}{W_i} = c_{e,i} + c_g (1 - \mu_i C_{p,i}) \tag{4}$$

where c_i is the electricity generation cost of the main power source, $c_{e,i}$ is the conventional electricity generation cost estimates of the main power source, and c_g is the electricity generation cost of the gas turbines. Therefore, the performance indicators, such as CF and AF, of the main power source must be analyzed to estimate the external cost for additional gas-turbine installation, based on Eq. (4). The CF is defined as the net actual generation (NAAG) that is produced by a generating unit in a given period as a fraction of the net maximum generation (NMG) [5].

$$CF = \left(\frac{NAAG}{NMG} \right) \times 100\% \tag{5}$$

where the NAAG is the energy that is generated by a unit in a given period and the NMG is the energy that could be produced by the unit in the given period if it were to operate continuously at maximum capacity. The AF is defined as the fraction of a given operating period in which a generating unit is available without any outages [5]:

$$AF = \left(1 - \frac{POH + UOH}{PH} \right) \times 100\% \tag{6}$$

where the planned outage hours (POHs) are the number of hours for which a unit is in a standard or extended planned outage state. The unplanned outage hours (UOHs) are the number of hours a unit is in a Class 0, Class 1, Class 2, or Class 3 or in maintenance outage states, whereas the period hours (PHs) are the number of hours a unit is in the active state.

2.2. Accident-consequence analysis

In this study, to quantitatively assess the consequences of various accident scenarios, the public health risk was

estimated by considering the possible accident scenarios for NPPs, solar PV systems, and WTGs based on probabilistic risk assessment (PRA) methodology. To ensure that the public health risk of each scenario for each type of power source was assessed based on the same criteria, the area of interest in which the public health risk was assessed was defined for each power source. It was assumed that for each energy source, the same capacity of 1,000 MW could be achieved with a uniform installation of facilities within a certain area of up to 20 km in radius; then, the equivalent radius of the area of interest for each power source could be defined as follows by considering the rated power output of each power source:

$$\frac{\pi\,(20\ \mathrm{km})^2}{\pi r_e^2} = \frac{1{,}000\ \mathrm{MW}}{P_r} \tag{7}$$

where r_e is the equivalent radius of the defined area of interest, A, and P_r is the rated power output of each power source. Based on the identified area of interest, the average individual health risk can be estimated by multiplying the accident frequency by the ratio of the number of equivalent fatalities to the total population residing inside the defined area of interest. Because each energy source has a different rated power output, the average individual health risk per terawatt-hours (TWh) of electricity that is annually produced by each energy source is estimated

$$\text{Average individual health risk per terawatt-hours of electricity} = \frac{\text{Average individual health risk}}{\text{Annual electricity production}} \tag{8}$$

$$\text{Average individual health risk} = \sum_i P_i \cdot \frac{HEC_i}{POP_{tot}} \tag{9}$$

$$HEC_i = \iint_A \text{fatality risk}_i \cdot \rho_{pop}\, dx\, dy \tag{10}$$

$$POP_{tot} = \iint_A \rho_{pop}\, dx\, dy \tag{11}$$

where P_i is the frequency of the specified accident scenario; HEC_i is the number of cases of potential health effects resulting in fatality for the nearby population, which is calculated as the product of the fatality risk and the population density, ρ_{pop}, inside the area of interest, A, for various accident scenarios, i; and POP_{tot} is the total population residing within the area of interest, which is considered to have the same population density, ρ_{pop}, for each energy source.

3. Analysis

3.1. Power-uncertainty analysis

3.1.1. Nuclear power plants

To assess the CF of NPPs, stochastic analysis was conducted based on historical data regarding the CFs of NPPs operating in Korea over the past 2 decades, according to the International Atomic Energy Agency Power Reactor Information System database [6].

To assess the AF of NPPs, both the planned outage time required for overhaul processes and the unplanned outage time attributable to unplanned reactor trip events were considered. To estimate the planned outage time, the general overhaul processes for the NPPs were considered. Typically, planned overhaul processes, which include maintenance tasks and tests of various NPP components, are performed at regular intervals, which is generally 1 month of planned overhaul for every 18 months of operation.

To estimate the unplanned outage time, a list of major events was collected, including unplanned reactor trips that have occurred in Korean NPPs as logged in the Operational Performance Information System provided by the Korea Institute of Nuclear Safety [7]. To estimate the outage time attributable to unplanned reactor trip events, detailed information was collected regarding the outage time for every primary cause of unplanned reactor events. The outage time was calculated as the difference between the date of the event and the date when operation resumed for each of the 349 data sets collected concerning unplanned reactor trip events, excluding events that occurred during planned overhaul periods. The data were regressed into a log-normal distribution based on the probability-density function of the outage-time data for each event.

The histogram of the collected outage-time data for each primary cause is presented in Fig. 1. Detailed log-normal parameters for each primary cause are summarized in Table 1. Based on this analysis of the estimated mean failure-rate and log-normal outage-time fit parameters for each primary cause, the unplanned outage times associated with the various NPP failure modes were estimated based on Monte Carlo simulations, and the AF of NPP was then calculated using Eq. (6).

3.1.2. Solar PV systems

Predicting the performance of residential PV cells and panels requires knowledge of the behavior of the climatic factors, such as the annual amount of solar radiation. The solar insolation at a given geographical location depends on the Earth's daily rotation, the Earth–Sun distance, and the Earth's axial tilt relative to the Sun [8]:

$$W = S_0 \cos z = S_0(\sin\theta \sin\delta + \cos\theta \cos\delta \cos H) \tag{12}$$

where W is the solar energy flux at the Earth–Sun distance; S_0 is the solar constant; z is the solar zenith angle, which is a function of the latitude, θ, the solar declination, δ, and the hour angle of the Sun, H. Using Eq. (12), the annual solar insolation in Korea was calculated by modeling the change in the daily obliquity, declination, and hour angle throughout the year. Because the solar insolation is also affected by climatic changes, such as the amount of cloud cover, the annual solar insolation intensity was calculated by multiplying the estimated hourly solar insolation by the average yearly clearness index observed in Korea. The detailed parameters used to simulate the yearly solar insolation at ground level are provided in Table 2.

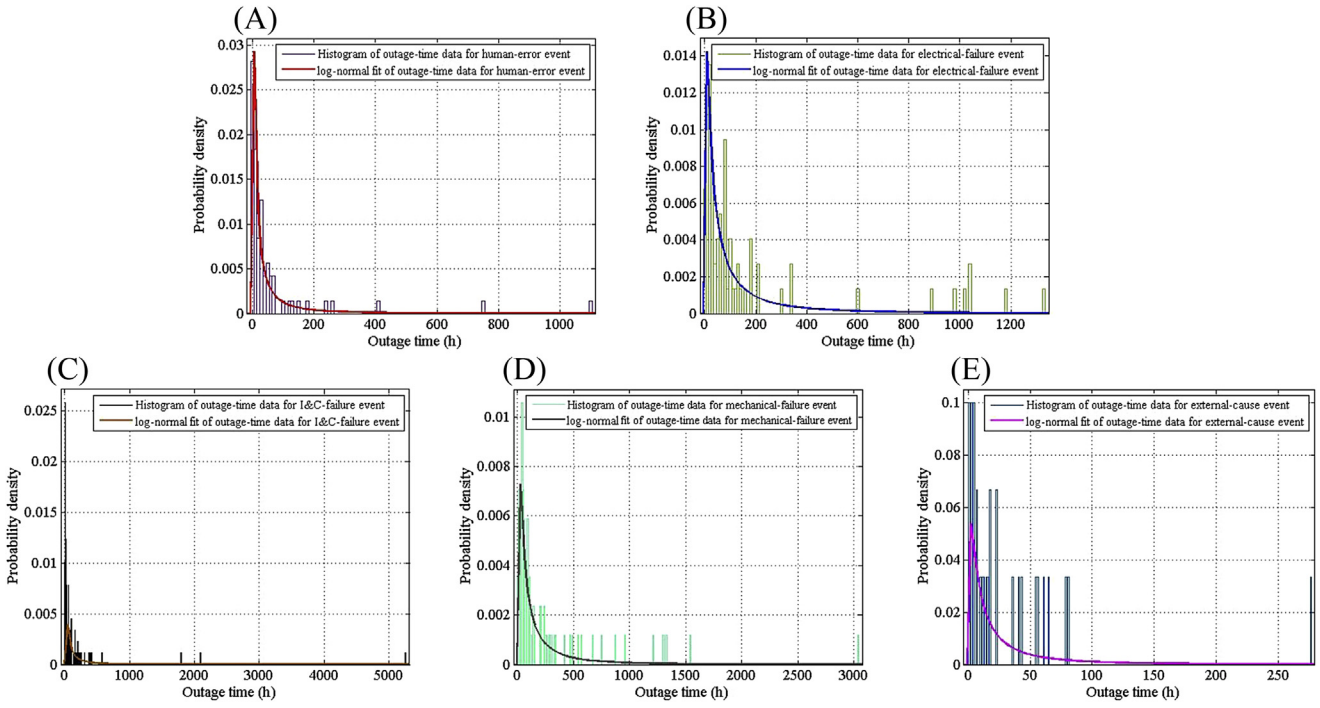

Fig. 1 – Histograms and log-normal regressions of the outage time caused by unplanned reactor trip events for various primary causes: (A) human error, (B) electrical failure, (C) instrumentation failure, (D) mechanical failure, and (E) external cause.

To analyze the power output of solar cells depending on the incident solar insolation, a simple electrical circuit diagram of a typical solar cell was modeled using a current source in parallel with a diode, as illustrated in Fig. 2 [10]. Based on the PV-cell circuit diagram, the net current in the cell can be derived as follows:

$$I = I_L - I_0\left[e^{\frac{q(V+IR_S)}{nkT}} - 1\right] \tag{13}$$

Table 1 – Log-normal regression parameters of the outage-time data for each primary cause.

Cases	μ (location parameter)	σ (scale parameter)	Mean (h)
Human error	2.67	1.85	80.07
Electrical failure	4.03	1.57	192.06
Instrumentation failure	3.35	1.90	174.43
Mechanical failure	4.45	1.50	262.73
External cause	2.64	1.41	37.82

Table 2 – Meteorological parameters for the simulation of annual solar irradiance.

Parameter	Value
Solar constant (W/m^2)	1,377
Latitude (degrees)	37°57′
Maximum/minimum declination (degrees)	±23.5
Clearness index (%) [9]	63.6

$$I_L = I_{SC}\frac{G}{G_{ref}} \tag{14}$$

$$I_0 = \frac{I_{SC}}{\left(e^{\frac{qV_{OC}}{nkT}} - 1\right)} \tag{15}$$

$$R_S = -\frac{dV}{dI_{V_{OC}}} - \frac{1}{X_V} \tag{16}$$

$$X_V = I_0\frac{q}{nkT}e^{\frac{qV_{OC}}{nkT}} - \frac{1}{X_V} \tag{17}$$

where I is the net current in the cell, which is determined by the photocurrent, I_L, the saturation current of the diode, I_0, and the electrical characteristics of a solar PV module, such as the operating voltage of the cell, V, diode quality factor, n, surface temperature of the cell, T, and the series resistance in

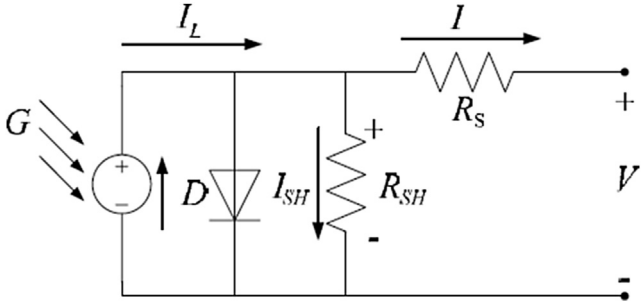

Fig. 2 – Schematic of the simple electrical circuit used to model a solar photovoltaic cell.

the cell, R_s. The photocurrent is directly proportional to the short-circuit current, I_{SC}, and the ratio of incident solar irradiance, G, to reference solar irradiance, G_{ref}.

In this study, we assume the use of the Solarex MSX-60 PV module (Solarex, Frederick, MD, USA), which is one of the most widely used modules for residential solar PV systems [11]. The series resistance considered in the model was used to solve for the net current in the cell based on the electrical characteristics of the module using the Newton–Raphson method, and the characteristic I–V curve of a single solar PV module was derived based on the net current in the circuit, depending on the operating voltage. In this analysis, the residential 5-kWp solar PV system consisting of eight series with 10 parallel circuits of PV modules (8-by-10) was considered. Based on the calculated yearly solar insolation data, the derived power curve and the annual power output of the residential solar PV array were estimated, and the mean CF was then calculated using Eq. (5).

Although the performance of a solar PV system varies based on irradiance and module performance, it can also experience component failure or outage during operation. To analyze the AF of solar PV systems, reliability data were collected for the components of the solar PV system. The outage time attributable to the failure of these components was estimated using the failure-rate and repair-time data for major components, including the PV module array, the string, the combiner box, the inverter, the alternating current disconnect, and the grid connection. To calculate the outage time attributable to unexpected failures of the components, the failure-rate and repair-time data for each component of the solar PV system were prepared based on the input data for the PV reliability and performance model developed by Sandia National Laboratories [12]. To assess the average annual unplanned outage time of a solar PV system caused by component failure, a Monte Carlo simulation was conducted to estimate the yearly outage time, which was calculated as the sum of the repair times associated with the failure of each component. Based on the outage time thus estimated, the AF of the system was calculated using Eq. (6).

3.1.3. *Wind-turbine generators*

The power output of a WTG is influenced by the random nature of the incident wind velocity, which is generally represented by the Weibull distribution [13]. To obtain yearly wind-speed data, the wind information recorded at the Gosan site, which has the highest recorded wind speed in Korea as shown in Table 3, was used for the analysis.

Typically, wind-turbine power production depends on the energy contained in the wind. The following second-order function of the wind-speed variable was used in this analysis to simulate the power output performance for WTGs [15]:

$$\begin{aligned} P(v) &= 0 \quad 0 \le v < v_{ci} \\ &= (A + Bv + Cv^2)P_r v_{ci} \le v < v_r \\ &= P_r v_r \le v < v_{co} \\ &= 0 \quad v \ge v_{co} \end{aligned} \tag{18}$$

where v_{ci} is the cut-in wind speed, v_r is the rated output wind speed, at which the actual power output reaches the rated power output, P_r. At higher wind speeds, the turbine is designed to limit the power output to this maximum level. v_{co} is the cut-out speed at which a braking system is activated to bring the rotor to a standstill. The constants A, B, and C can be derived as functions of the aforementioned parameters, based on the technical specifications of a given WTG. In this study, the power curve was modeled based on the technical specifications of the Siemens SWT-2.3-93 wind turbine (Siemens AG, Erlangen, Germany), which are presented in Table 4. Using the simulated annual wind-speed data and the derived power-curve equation, the CF of WTG was calculated based on Eq. (5).

Table 3 – Weibull distribution parameters of wind velocities observed at the Gosan station [14].

Parameter	Value
k (shape parameter)	8.69
λ (scale parameter)	1.65
Mean wind speed (m/s)	7.77

Because a WTG is composed of various mechanical components, including rotor blades, a gearbox, and a generator, it can experience component failure or outages during operation caused by a variety of factors, including mechanical stresses and abnormally high wind speeds. Therefore, the reliability data for the components, which comprise a wind turbine, were collected from the German 250-MW Wind Monitoring Campaign database of observed turbine reliabilities and the failure rate of each component [17]. The failure-rate data for turbines with a capacity of >1 MW at low, moderate, and high wind speeds were used for the reliability analysis, whereas the repair time for each component was assumed to be deterministic and independent of the wind speed, as shown in Table 5. To estimate the outage time attributable to failures and subsequent repair during 1 year of operation, a Monte Carlo simulation was conducted and the AF was calculated using Eq. (6).

3.2. *Accident-consequence analysis*

3.2.1. *Nuclear power plants*

When severe NPP accidents occur, some fraction of the radionuclides may be released into the environment, and the transported radionuclides can adversely affect human health. The assessment of the public health risk associated with the accidental release of radioactive materials from an NPP accident requires the following: (1) identifying the quantities of by-products released by the nuclear fission reaction; (2) specifying the release profile and site-specific data; (3) simulating the airborne transport of the released radioactive materials; and (4) analyzing the response of the exposed population for various exposure pathways.

Table 4 – Technical specifications of the Siemens SWT-2.3-93 turbine [16].

Parameter	Value
Nominal power (MW)	2.3
Cut-in wind speed (m/s)	3
Rated wind speed (m/s)	14
Cutout wind speed (m/s)	25

Table 5 – Failure frequency depending on wind velocity and repair time for each wind-turbine component [18].

Component	Electrical system	Electronic control	Sensors	Hydraulic system	Yaw system	Rotor blades	Mechanical brake	Rotor hub	Gearbox	Generator	Support structure/ housing	Drive train
Failure frequency at low wind (/y)	0.83	0.62	0.37	0.35	0.27	0.26	0.20	0.16	0.15	0.14	0.13	0.08
Failure frequency at mid wind (/y)	2.00	1.49	0.89	0.85	0.66	0.63	0.48	0.40	0.36	0.33	0.32	0.19
Failure frequency at high wind (/y)	3.00	2.23	1.34	1.28	1.00	0.94	0.72	0.60	0.54	0.50	0.49	0.28
Repair time (d)	1.80	2.30	1.80	1.40	3.30	5.10	3.30	4.40	7.90	9.30	4.10	7.10

To specify the core inventory, source-term information for a hypothetical NPP accident was determined based on a Level 2 probabilistic risk assessment (PRA) analysis for conventional 1,000-MW NPPs. In this study, a steam-generator tube-rupture accident under containment-bypass conditions was assumed to determine the release fraction of each chemical group, as shown in Table 6. In this analysis, the radioactive materials were assumed to be released at ground level, and the plume containing these materials was assumed to continue to disperse throughout the environment for 1 day. A common dry deposition velocity of 0.01 m/s, corresponding to unfiltered release directly into the environment, was assumed [19].

Meteorological conditions and population distribution near the NPP site are important when simulating the airborne transport of released radionuclides and estimating the public health effect. Therefore, the yearly meteorological data observed at the Kori NPP site in Korea were used as input data to simulate the atmospheric transport of the released radionuclides using a stratified random sampling method for the case study [21]. For the population data, it was assumed that the population is uniformly residing at a distance of >8 km from the site. The population density was assumed according to the estimate for Korea.

For the simulation of the airborne transport of gaseous radioactive materials released into the environment, the Gaussian plume model was used. To analyze the response of the population exposed to transported radionuclides, the MELCOR Accident Consequence Code System 2 [22], developed by Sandia National Laboratories, was used. In this analysis, mitigative action during the emergency phase was addressed by simulating the radial evacuation of the population with an evacuation speed of 1.8 m/s [19].

3.2.2. *Solar PV systems*

For the consequence analysis of solar PV systems, the public health effects of a fire in a 5-kWp residential cadmium telluride (CdTe) PV system were examined. Cadmium is considered a probable human carcinogen, classified as a Group B1

Table 6 – Release fraction of radionuclide for hypothetical nuclear power plant accident considered in this study [20].

Parameter		Value
Release fraction for each chemical group	Xe group (Kr, Xe)	9.50×10^{-01}
	I group (I)	1.30×10^{-01}
	Cs group (Rb, Cs)	1.30×10^{-01}
	Te group (Sb, Te)	4.90×10^{-01}
	Sr group (Sr)	8.60×10^{-04}
	Ru group (Co, Mo, Tc, Ru, Rh)	4.60×10^{-02}
	La group (Y, Zr, Nb, La, Pr, Nd, Am, Cm)	1.90×10^{-04}
	Ce group (Ce, Np, Pu)	7.10×10^{-04}
	Ba group (Ba)	1.40×10^{-02}

Am, Americium; Ba, Barium; Ce, Cerium; Cm, Curium; Co, Cobalt; Cs, Cesium; I, Iodine; Kr, Krypton; La, Lanthanum; Mo, Molybdenum; Nb, Niobium; Nd, Neodymium; Np, Neptunium; Pr, Praseodymium; Pu, Plutonium; Rb, Rubidium; Rh, Rhodium; Ru, Ruthenium; Sb, Antimony; Sr, Strontium; Tc, Technetium; Te, Tellurium; Xe, Xenon; Y, Yttrium; Zr, Zirconium.

carcinogen by the U.S. Environmental Protection Agency (EPA), and the chronic inhalation of or oral exposure to cadmium can lead to a build-up in the kidneys, causing kidney disease [23]. An assessment of the public health risk associated with the release of carcinogenic material from CdTe PV modules during a fire requires the following: (1) specifying the quantity of cadmium present in a residential CdTe PV module; (2) identifying the toxic chemicals released during a fire; (3) simulating the atmospheric transport of the released toxic substances; and (4) analyzing the response of the exposed population for defined exposure pathways.

To analyze the source term, the amounts of Cd and Te released were assumed to constitute 0.5% of the total CdTe material present in the PV module, as a conservative estimate [24]. To simulate the atmospheric transport of the released cadmium, the Gaussian plume dispersion model was used to estimate the ground-level concentration of toxic materials. To produce a conservative analysis, the worst-case meteorological conditions (Pasquill atmospheric stability of Class F, constant wind velocity of 1 m/s, and ground-level release) were assumed. The specific release description for a fire incident involving CdTe PV modules was defined as summarized in Table 7.

To analyze the response of the exposed population near the point of release, the critical exposure pathway was assumed to be via oral ingestion of ground-deposited cadmium, because a short-release duration was defined for the toxic-substance release. Therefore, a cancer risk evaluation method proposed by the U.S. EPA, which defines the quantitative relationship between dose and response using a cancer slope factor, was used to analyze the public health risk [26]. Based on the cancer slope factor for the oral ingestion of the cadmium, the cancer risk was computed for each age interval as follows:

$$\mathrm{Risk_i} = \mathrm{C} \times \frac{\mathrm{IR_i} \times \mathrm{EF_i} \times \mathrm{ED_i}}{\mathrm{BW_i} \times \mathrm{AT}} \times \mathrm{SF} \times \mathrm{ADAF_i} \tag{19}$$

where C is the concentration of the toxic chemical in the soil, IR is the ingestion rate of the contaminated environmental medium, EF is the exposure frequency, ED is the exposure duration, BW is the body weight, AT is the average time, which specifies the length of time over which the average dose is calculated, SF is the oral-ingestion cancer slope factor, and ADAF is an age-dependent adjustment factor for a given age interval, i. Based on the standard default exposure parameters for reasonable maximum exposure for resident cancer risk, as recommended by the U.S. EPA, the public health risk was estimated as the cancer risk of an adult for 50 years of exposure to the deposited cadmium [26].

Table 7 – Release description of toxic materials from a residential CdTe PV module.

Parameter	Value
Wind velocity (m/s)	1
Release duration (min)	15
Amount of CdTe in 5-kWp residential solar PV array (kg) [25]	0.6
Release fraction of CdTe inside solar PV array (%) [24]	0.5

CdTe, cadmium telluride; PV, photovoltaic.

3.2.3. *Wind-turbine generators*

In the case of WTG accidents, the consequence analysis was conducted focusing on the whole-blade failure WTG accident scenario, which may cause fatal effects due to the direct impact of blade fragments and subsequent blunt trauma. The assessment of the public health risk associated with whole-blade failure accidents in WTGs requires the following: (1) identifying the specifications of typical wind-turbine blades; (2) describing the release pattern of the blade fragment; (3) simulating the fragment's trajectory from the WTG to nearby populations; and (4) assessing the human vulnerability to a blade fragment generated by wind-turbine failure.

In this study, blade breakdown for a typical utility-scale wind turbine was investigated. The specifications of the considered wind turbine, including descriptions of the blades and rotors, are provided in Tables 8 and 9. Because whole-blade failure was assumed in this analysis, the total mass and full length of the blade were used for a conservative assessment of the public health risk. To simulate the random nature of the blade-detachment conditions, several parameters were assumed to have certain specific distributions, as indicated in Table 9.

To simulate the fragment's trajectory from the initial position of detachment from the WTG, under the assumption of flat terrain around the WTG site, a blade-throw model was developed considering the aerodynamic forces applied to the blade fragment. Three nonlinear, second-order coupled differential equations of motion can be modeled as follows, by considering the two important forces, which are the gravitational force and the drag force associated with air resistance in three-dimensional space, assuming that the wind rose is always perpendicular to the blade plane:

$$-\mathrm{F_D}\overrightarrow{v_x} = m\frac{d^2x}{dx^2} \tag{20}$$

$$-\mathrm{F_D}\overrightarrow{v_y} = m\frac{d^2y}{dy^2} \tag{21}$$

$$-mg - \mathrm{F_D}\overrightarrow{v_z} = m\frac{d^2z}{dz^2} \tag{22}$$

$$\overrightarrow{v_x} = \frac{v_x}{v}, \overrightarrow{v_y} = \frac{v_y}{v}, \overrightarrow{v_x} = \frac{v_z}{v}, v = \sqrt{v_x^2 + v_y^2 + v_z^2} \tag{23}$$

As implied by Eqs. (20–22), the horizontal trajectory of the projectile through the air depends on the drag force, which can be expressed in terms of several parameters:

$$F_D = C_D A_f \rho_{air} \frac{v^2}{2} \tag{24}$$

Table 8 – Technical specifications of the representative wind turbine considered for the accident-consequence analysis [16].

Parameter	Value
Hub height (m)	80
Rotor diameter (m)	93
Length of blade (m)	45
Blade's center of gravity distance from rotor center (m)	25.5
Blade mass (kg)	6,600

Table 9 – Assumptions of the parameters for release description of the blade fragment.

Parameter	Value
Exposed area (m^2)	Uniform distribution (Min. = 9.7, Max. = 96.8)
Coefficient of drag (unitless)	1
Angle of detachment (degree)	Uniform distribution (Min. = 0 Max. = 360)
Rotor speed (rpm)	Beta distribution (Min. = 14.5, Mode = 16.1, Max. = 38.6)
Wind speed (m/s)	Weibull distribution (Mean = 24)
Air density (kg/m^3)	1.225

Max., maximum; Min., minimum.

where A_f is the frontal surface area of the projectile, ρ_{air} is the density of the air, C_D is a dimensionless drag coefficient, and v is the relative velocity of the blade in the rest frame of the wind. Using the set of blade-fragment release conditions described in Tables 8 and 9, Eqs. (20–24) were integrated and solved numerically using a Runge–Kutta algorithm until the mass center of the blade fragment collided with the ground to simulate the ground-impact point of the blade. Several assumptions were made in this calculation: the blade fragment was represented by a point mass, the drag coefficient was held constant throughout the flight of the blade fragment, and the wind direction was assumed to be constant during the fragment's flight.

To assess the public health risk associated with wind-turbine blade failure, the direct impact of the blade fragment on a member of the nearby population was analyzed using the energy-based Blunt Criterion model [27]. The Blunt Criterion model is used to calculate the potential risk of an impact injury based on certain parameters and is defined as follows:

$$BC = \ln\left(\frac{\frac{1}{2}MV^2}{W^{\frac{1}{3}}TD}\right) \tag{25}$$

where M is the mass of the projectile in kg, V is the velocity of the projectile in m/s, W is the mass of the struck individual in kg, T is the combined thickness of the body wall at the impact location on the struck individual in cm, and D is the diameter of the projectile in cm. In this analysis, the average anthropometric characteristics of a human were used for the Blunt Criterion model [28]. Based on this model, the probabilities of producing injuries at all levels of injury severity, as determined by the Abbreviated Injury Scale (AIS), can be quantitatively estimated using the following logistic function [27]:

$$p = \frac{1}{1 + e^{-(a+b\times BC)}} \tag{26}$$

where p is the probability of injury at a certain AIS level caused by blunt trauma, BC is the Blunt Criterion value, and both a and b are coefficients whose values depend on the AIS level and the body part of concern. In this study, blunt trauma to the thorax was considered and an AIS level of 6, which denotes the highest severity of injury (an untreatable injury or fatality), was used to estimate the probability of fatality.

4. Results

4.1. Power-uncertainty analysis

The performance indicators, such as CF and AF, of the given energy sources can be used to estimate the external cost for additional gas-turbine installation associated with the energy source, and these performance indicators in the case of NPPs, solar PV systems, and WTGs were analyzed using the standard definition for electric generating units—see Eqs. (5) and (6). Based on the proposed framework in this study, the mean CF and mean AF were estimated, respectively, for each energy source, and the results are presented in Table 10.

According to the estimated performance indicators of each energy source, the necessary power output of the gas-turbine power plants used for backup power generation to compensate for deficient power output during the normal operation of each energy source can be derived using Eq. (4). The electricity generation cost for a conventional liquefied natural gas power plant in Korea, in the year 2012, was 168.1 won/kWh (14.9 U.S. cents/kWh), and this was used as the electricity generation cost for the gas turbines [29]. The additional external costs for the gas-turbine power for each energy source is estimated, as summarized in Table 11.

4.2. Accident-consequence analysis

According to the accident-consequence analysis, the average individual health risks of NPPs, solar PV systems, and WTGs were estimated based on the predefined accident scenarios considered for each case. For each energy option, the same

Table 10 – Estimated mean capacity factor and availability factor for each energy source.

Parameter	NPP	Solar photovoltaic system	WTG
Mean capacity factor (%)	89.11	16.98	28.71
Mean availability factor (%)	93.06	89.11	91.59

NPP, nuclear power plant; WTG, wind-turbine generator.

Table 11 – Electricity generation costs considering the power uncertainty of each energy source.

Parameter	NPP	Solar photovoltaic system	WTG
Conventional electricity generation cost estimate (U.S. cents/kWh) [1]	11.4	15.4–17.8	11.9–22.2
Additional external cost for gas-turbine power (U.S. cents/kWh)	2.5	12.6	11.0
Electricity generation cost (U.S. cents/kWh)	13.9	28.0–30.4	22.9–33.2

NPP, nuclear power plant; WTG, wind-turbine generator.

population density of 485.6 residents/km^2 was assumed, with a uniform population distribution in the defined area of interest; this value was adopted from the estimated average population density of Korea in the year 2010 [30].

In the case of a hypothetical NPP accident, the exceedance probability as a function of the number of each type of health-effect case was obtained as shown in Fig. 3, considering the rated power output of a conventional 1,000-MW NPP. Thus, the average individual health risk was calculated as the sum of the grand mean of early fatality cases and latent cancer fatality cases divided by the total population, under the assumption of a population residing between 8 km and 20 km from the NPP site.

In the case of solar PV systems, the cancer risk profile was obtained, as shown in Fig. 4, for distances from the point of release up to the equivalent radius of 45 m; this profile was estimated using Eq. (7), considering the rated power output of a conventional 5-kWp residential solar PV module. Thus, the average individual health risk was calculated as the total number of incidences of chronic cancer fatality caused by oral ingestion of deposited Cd, divided by the total population residing in the area of interest, up to 45 m from the point of release of cadmium from inside the CdTe PV module.

In the case of whole-blade-throw accidents in WTGs, the probability contour for fatality caused by blunt trauma was obtained as shown in Fig. 5 for the distance from the point of release up to the equivalent radius of 960 m, which was estimated using Eq. (7) based on the rated power output of a typical utility-scale WTG, 2.3 MW. Thus, the average individual health risk was calculated as the total number of fatalities caused by blunt trauma from a thrown blade fragment, divided by the total population residing in the area of interest, up to 960 m from the WTG site.

Based on the estimated average individual health risk of each energy source, the risk per terawatt-hours of electricity produced by each energy source was estimated using Eq. (8) by considering the accident frequency, as described in Table 12, and the rated annual power production for each energy source. The results are presented in Table 13.

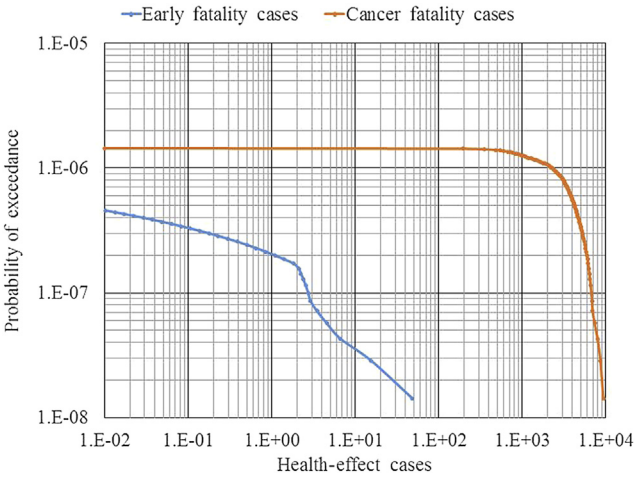

Fig. 3 – Exceedance probability as a function of the number of each type of health-effect case for a hypothetical nuclear power plant accident.

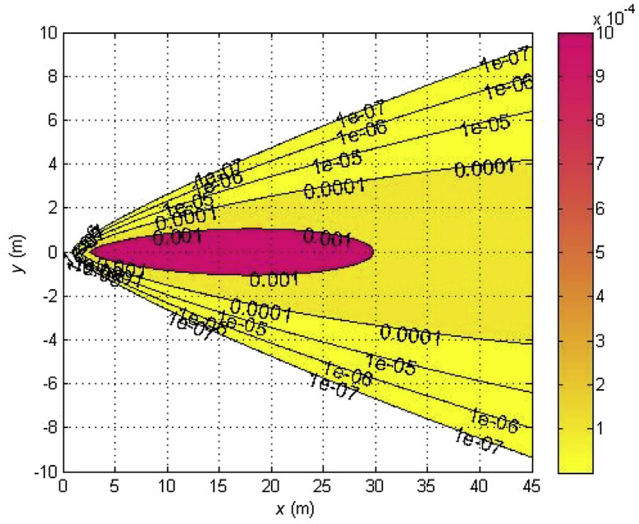

Fig. 4 – Cancer risk profile associated with the ingestion of soil contaminated with ground-deposited cadmium for a cadmium telluride (CdTe) solar photovoltaic fire accident scenario.

5. Discussion

As previously discussed, the social cost of providing protective measures for a power-distribution system to compensate for power-source instability, especially in the case of renewable energy sources, is typically ignored when calculating the electricity generation cost. The results indicate that compared with the conventional electricity generation cost estimates for each energy source, the social cost of gas-turbine installation plays a dominant role in determining the electricity generation cost, especially in the case of renewable energy sources.

Although the accident-consequence analysis results indicate a lower average individual health risk per terawatt-hours

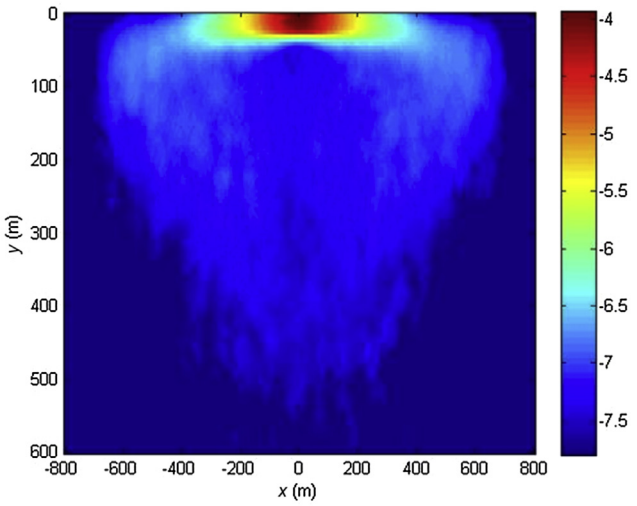

Fig. 5 – Probability contour for fatality caused by blunt trauma for the whole-blade failure accident scenario (in logarithmic scale).

Table 12 – Accident frequencies for the specified accident scenarios for each energy source.

Energy source	Accident frequency (/y)	Description
NPP	1.43×10^{-06}	Large early release frequency for steam-generator tube-rupture accidents under containment-bypass conditions [20]
CdTe solar photovoltaic system	1.00×10^{-04}	The probability of residential fires in wood-frame houses in the United States [23]
WTG	5.40×10^{-03}	Failure data observed from 2000 to 2003, as reported in an Alameda County study [31]

CdTe, cadmium telluride; NPP, nuclear power plant; WTG, wind-turbine generator.

of electricity for NPPs compared with solar PV systems and WTGs, as shown in Table 13, the risk perception and risk aversion of the public must be considered when assessing the cost of accident-risk response, which is a hidden cost of an energy system. By comparing the estimated average individual health risk, shown in Table 13, and the accident frequency of the initiating accident event of each energy source, shown in Table 12, the contribution of the assumed initiating event frequency to the average individual health risk in the case of a renewable energy source is large compared with the case of NPP. This infers that the risk aversion must be considered when estimating the external cost for an NPP accident because this can be categorized as a group accident, which occurs with a low probability but incurs severe consequences [32]. In principle, the public tends to behave in a risk-averse manner, lending more weight to, and expending more societal resources on, measures to prevent a group accident. In particular, the value of statistical life depends on how individuals perceive mortality risks and their perceptions of baseline risks and changes in probability. For instance, if the public perceives the risk to be higher than the true risk, then monetary estimates of the value of risk reduction are expected to be higher, resulting in the estimation of a higher accident-risk response cost than the expected cost. Therefore, future work will include an investigation of public risk aversion to allow the social acceptability of the accident risk to be considered in the calculation of these external costs and of the parameters, which were assumed conservatively and used as an input data in this analysis, to allow more realistic analysis for more accurate estimation of the accident-risk response costs associated with various energy sources.

Table 13 – Average individual health risk per terawatt-hours (TWh) of electricity produced by each energy source.

Parameter	NPP	Solar photovoltaic system	WTG
Average individual health risk (/y)	9.82×10^{-09}	1.23×10^{-11}	1.18×10^{-09}
Annual rated power output (TWh/y)	8.76×10^{00}	4.38×10^{-05}	2.02×10^{-02}
Average individual health risk per TWh of electricity produced (/TWh)	1.12×10^{-09}	2.82×10^{-07}	5.86×10^{-08}

NPP, nuclear power plant; WTG, wind-turbine generator.

6. Conclusions

In response to the Fukushima Daiichi NPP accident, the Japanese government published a report regarding cost estimations, which revealed the existence of hidden costs for various power generation sources. However, this report failed to consider the social costs of providing measures to protect the power-distribution networks from power-source instability and the cost of accident-risk response for renewable energy sources. Therefore, an integrated framework for power-uncertainty analysis and accident-risk analysis for NPPs, WTGs, and solar PV systems is proposed to incorporate these risks into estimates of the social costs of various power sources.

For the power-uncertainty analysis, the required capacity of a gas-turbine power plant to be used as the backup power source to compensate for fluctuations in the output of the main power source was estimated. The annual power output and the annual outage time associated with the failure of system components were simulated, and based on the results, the performance indicators (CF and AF) for each power plant were derived. For the accident-consequence analysis, the average individual health risk per terawatt-hours of electricity produced by each energy source was estimated by considering the accident frequency and potential public health-effect cases based on the specific accident scenarios considered for each energy source. The results indicated a significant contribution of the intermittency-compensation cost compared with the conventional electricity generation cost estimates; this contribution was relatively large in the case of renewable energy sources compared with the case of NPPs. This finding implies that neglecting the intermittency-compensation costs of renewable energy sources would be a serious omission, especially at higher penetration levels. In terms of accident risk, the estimated average individual health risk per terawatt-hours of electricity produced in the case of NPPs was less than in the case of renewable energy sources.

However, the sociological aspects of the public perception of risk must be taken into account along with the estimated accident risk to accurately analyze the cost of accident-risk response for each energy source. Therefore, future work will include detailed economical evaluations of the accident risks investigated in this study, and will assess the economic feasibility of each energy option.

Conflicts of interest

All contributing authors declare no conflicts of interest.

Acknowledgments

This work was supported by the 'Valuation and Socioeconomic Validity Analysis of Nuclear Power Plants In Low Carbon Energy Development Era' of the Korea Institute of Energy Technology Evaluation and Planning, granted by the Ministry of Trade, Industry and Energy of the Republic of Korea. 20131520000040.

REFERENCES

[1] Y. Matsuo, Summary and Evaluation of Cost Calculation for Nuclear Power Generation by the Cost Estimation and Review Committee, Institute for Energy Economics, Tokyo, Japan, 2012.
[2] H.W. Lewis, R.J. Budnitz, W.D. Rowe, H.J.C. Kouts, F.V. Hippel, W.B. Loewenstein, F. Zachariasen, Risk assessment review group report to the US Nuclear Regulatory Commission, IEEE Trans. Nucl. Sci. 26 (1979) 4686–4690.
[3] T. Tsoutsos, N. Frantzeskaki, V. Gekas, Environmental impacts from the solar energy technologies, Energy Policy 33 (2005) 289–296.
[4] J.F. MacQueen, J.F. Ainslie, D.J. Milborrow, D.M. Turner, D.T. Swift-Hook, Risks associated with wind-turbine blade failures, IEEE Proc. A (Phys. Sci. Meas. Instrum., Manage. Educ. Rev.) 130 (1983) 574–586.
[5] Institute of Electrical and Electronics Engineers (IEEE), IEEE Standard Definitions for Use in Reporting Electric Generating Unit Reliability, Availability and Productivity, IEEE Standard 762, IEEE, New York, 2006.
[6] International Atomic Energy Agency [Internet]. Power Reactor Information System (PRIS), Vienna, Austria, 2014 [cited 2014 Aug 6]. Available from: http://www.iaea.org/pris/.
[7] Korea Institute of Nuclear Safety [Internet]. Operational Performance Information System (OPIS) Daejeon, South Korea, 2014 [cited 2014 Jul 24]. Available from: http://opis.kins.re.kr/.
[8] L.W. Meech, On the Relative Intensity of the Heat and Light of the Sun upon Different Latitudes of the Earth, vol. 9, Smithsonian Institution, Washington, DC, 1857.
[9] D.K. Jo, C.Y. Yun, K.D. Kim, Y.H. Kang, Revaluation of atmospheric clearness Index in Korea Peninsula, in: Proceedings of the Annual Autumn Conference of the Korean Solar Energy Society (KSES 2009), vol. 11, 2009, pp. 68–73.
[10] E. Lorenzo, Solar Electricity: Engineering of Photovoltaic Systems, Earthscan/James & James, London, 1994.
[11] California Solar Center [Internet]. Solarex MSX60 and MSX64 Solar Arrays Datasheet, MD, USA, 1997 [cited 2014 Jul 28]. Available from: http://www.californiasolarcenter.org/newssh/pdfs/solarex MSX64.pdf.
[12] P.M. Steven, E.G. Jennifer, S.S. Joshua, The Comparison of Three Photovoltaic System Designs Using the Photovoltaic Reliability and Performance Model (PVRPM), Rep. No. SAND2012-10342, Sandia National Laboratories, Albuquerque, NM, 2012.
[13] J.V. Seguro, T.W. Lambert, Modern estimation of the parameters of the Weibull wind speed distribution for wind energy analysis, J. Wind. Eng. Ind. Aerodyn. 85 (2000) 75–84.
[14] D.W. Kim, H.R. Byun, Spatial and temporal distribution of wind resources over Korea, J. Atmos. 18 (2008) 171–182.
[15] P. Giorsetto, F.U. Kent, Development of a new procedure for reliability modeling of wind turbine generators, IEEE Trans. Power Appar. Syst. 1 (1983) 134–143.
[16] A.G. Siemens, Siemens Wind Turbine SWT 2.3-93 Brochure, Berlin, Germany, 2009.
[17] E. Echavarria, B. Hahn, G.J. van Bussel, T. Tomiyama, Reliability of wind turbine technology through time, J. Sol. Energy Eng. 130 (2008) 031005.
[18] S.R. Arwade, A.L. Matthewand, D.G. Mircea, Probabilistic models for wind turbine and wind farm performance, J. Sol. Energy Eng. 133 (2011) 041006.
[19] U.S. Department of Energy (DOE), MACCS2 Computer Code Application Guidance for Documented Safety Analysis, DOE-EH-4.2.1.4, U.S. Department of Energy, Office of Environment, Safety and Health, Washington, DC, 2004.
[20] T.W. Kim, J.J. Ha, S.H. Kim, J.T. Jeong, K.R. Min, K.Y. Kim, A Comparison Study on the Integrated Risk Estimation for Various Power Systems, Rep. No. KAERI/RR-2513, Korea Atomic Energy Research Institute, Daejeon, South Korea, 2007.
[21] B.H. Ha, Y.O.J.Y. Oh, S.J. Oh, Examination of the emergency planning zone (EPZ) using level 3 PSA approach with MACCS2, in: Transactions of the Korean Nuclear Society Autumn Meeting (KNS 2013-Autumn), vol. 2, 2013, p. 485.
[22] D.I. Chanin, M.L. Young, J. Randall, K. Jamali, Code Manual for MACCS2, in: User's Guide (SAND97-0594), vol. 1, Sandia National Laboratories, Albuquerque, NM, 1997.
[23] U.S. Environmental Protection Agency (EPA), Integrated Risk Information System (IRIS) on Cadmium, National Center for Environmental Assessment, Office of Research and Development, Washington, DC, 1999.
[24] V.M. Fthenakis, M. Fuhrmann, J. Heiser, A. Lanzirotti, J. Fitts, W. Wang, Emissions and encapsulation of cadmium in CdTe PV modules during fires, Prog. Photovoltaics: Res. Appl. 13 (2005) 713–723.
[25] P.D. Moskowitz, V.M. Fthenakis, Toxic materials released from photovoltaic modules during fires: health risks, Solar Cells 29 (1990) 63–71.
[26] U.S. Environmental Protection Agency (EPA), Proposed Guidelines for Carcinogen Risk Assessment, 17960–18011, U.S. EPA, Washington, DC, 1996.
[27] L.M. Sturdivan, D.C. Viano, H.R. Champion, Analysis of injury criteria to assess chest and abdominal injury risks in blunt and ballistic impacts, J. Trauma 56 (2004) 651–663.
[28] M. Frank, B. Bockholdt, D. Peters, J. Lange, R. Grossjohann, A. Ekkernkamp, P. Hinz, Blunt criterion trauma model for head and chest injury risk assessment of cal. 380 R and cal. 22 long blank cartridge actuated gundog retrieval devices, Forensic Sci. Int. 208 (2011) 37–41.
[29] C.H. Lee, External Costs of Nuclear Energy in Korea, Korea Environment Institute, Seoul, Korea, 2013.
[30] Statistics Korea (KOSTAT) [Internet]. Korean Statistical Information Service (KOSIS), Daejeon, South Korea, 2014 [cited 2014 Sep 25]. Available from: http://kosis.kr/.
[31] Larwood, Scott, C.P. Van Dam, Permitting setback requirements for wind turbines in California, California Wind Energy Collective, 2006.
[32] A. Luigi, P.C. Braga, R. Dal, Clean technology and the environment, Aerobiologia 11 (1995) 279.